

Deterministic SR in a Piecewise Linear Chaotic Map

Sitabhra Sinha ¹ and Bikas K. Chakrabarti ²

¹ Machine Intelligence Unit, Indian Statistical Institute, Calcutta 700 035, India.

² Saha Institute of Nuclear Physics, 1/AF Bidhan Nagar, Calcutta - 700 064, India.

Abstract

The phenomenon of Stochastic Resonance (SR) is observed in a completely deterministic setting - with thermal noise being replaced by one-dimensional chaos. The piecewise linear map investigated in the paper shows a transition from symmetry-broken to symmetric chaos on increasing a system parameter. In the latter state, the chaotic trajectory switches between the two formerly disjoint attractors, driven by the map's inherent dynamics. This chaotic switching rate is found to 'resonate' with the frequency of an externally applied periodic perturbation (multiplicative or additive). By periodically modulating the parameter at a specific frequency ω we observe the existence of resonance where the response of the system (in terms of the residence-time distribution) is maximum. This is a clear indication of SR-like behavior in a chaotic system.

PACS numbers:05.40.+j, 05.45.+b

"Stochastic Resonance" (SR) is a recently observed nonlinear phenomena in noisy systems, where the noise helps in amplifying a sub threshold signal (which would have been otherwise undetected) when the signal frequency is close to a critical value [1]. This occurs because of noise-induced hopping between multiple stable states of a system, locking on to an externally imposed periodic signal. A theoretical understanding of SR in bistable systems, subject to both periodic and random forcing, has been obtained based on the rate equation approach [2]. As the output of a chaotic process is indistinguishable from that of a noisy system, the question of whether a similar process occurs in the former case has long been debated. In fact, Benzi *et al* [1] indicated that the Lorenz system of equations, a well-known paradigm of chaotic behavior might be showing SR. Later studies [3], [4] in both discrete-time and continuous-time systems seemed to support this view. However, it is difficult to guarantee that the response behavior is due to "resonance" and not due to "forcing". In the latter case, the periodic perturbation is of so large an amplitude, that the system is forced to follow the driving frequency of the periodic forcing. The ambiguity is partly because the Signal-to-Noise Ratio (SNR) is a monotonically decreasing function of the forcing frequency and cannot be used to distinguish between resonance and forcing. In the present work this problem is avoided by measuring the response of the system in terms of the normalized distribution of residence times [5]. For SR, this measure shows non-monotonicity with the variation of both noise intensity and signal frequency.

Ippen *et al* [6] have used a chaotic driving term to show SR-like behavior in the SNR of the system response. However in this case the chaos is supplied from outside, and not inherent to the system. If SR is indeed used for information processing by biological systems, then it is likely that organs producing chaotic behavior might enhance their survival capability through selective amplification of signals in a noisy background. In this case, the inherent chaos of the system itself could play the role of "noise". In the model proposed in this paper, a simple one-dimensional map has been shown to use its inherent chaoticity to replicate SR-like phenomena. This suggests a deep relation between stochastic resonance on the one hand, and crises in chaotic dynamics on the other, mentioned in [7]. The present work also supports this view.

The simplest chaotic system to show SR-type behavior are one-dimensional maps with two critical points. The most commonly studied system of this kind is the cubic map [8],

$$x_{n+1} = ax_n^3 + (1-a)x_n,$$

where a is a tunable parameter. The map is found to consist of two attractors, the initial condition determining the attractor into which the system settles. Various properties of such ‘bimodal’ maps differ from those observed for the well-studied class of maps with a single critical point (e.g., the logistic map).

Recently, SR has been studied in 1-D maps with two well-defined states (but not necessarily stable) with switching between them aided by either additive or multiplicative external noise [9]. However, dynamical contact of two chaotic 1-D maps can also induce rhythmic hopping between the two domains of the system [10]. The present work shows how the chaotic dynamics of a system can itself be used for resonant switching between two states, without introducing any external noise.

The model chosen here is a piecewise linear bimodal map, henceforth referred to as the Discontinuous Anti-symmetric Tent (DAT) map, defined in the interval $[-1,1]$:

$$x(n+1) = F(x_n) \begin{cases} 1 + a(0.5 - x(n)), & \text{if } x(n) \geq 0.5 \\ 1 - a(0.5 - x(n)), & \text{if } 0 < x(n) < 0.5 \\ -1 + a(0.5 + x(n)), & \text{if } -0.5 < x(n) < 0 \\ -1 - a(0.5 + x(n)), & \text{if } x(n) \leq -0.5. \end{cases} \quad (1)$$

The map has a discontinuity at $x = 0$. The behavior of the system was controlled by the parameter a , ($0 < a < 4$). Onset of chaos occurs at $a = 1$. The chaos is symmetry-broken, i.e., the trajectory is restricted to either of the two sub-intervals R: $(0,1]$ and L: $(0,-1]$, depending on initial condition. Symmetry is restored at $a = 2$. The lyapunov exponent of the map is a simple monotonic function of the parameter a . The piecewise-linear nature of the map makes its behavior simpler to study than, say, the cubic map described above. The map is shown in fig. 1, the inset giving a detailed picture of the region around the discontinuity at $x = 0$. Fig. 2 shows the evolution of the map’s attractor with a increasing from 0 to 4.

The map has a symmetrical pair of fixed points $x_{1,2}^* = \pm \frac{1+a/2}{1+a}$ which are stable for $0 < a < 1$ and unstable for $a > 1$. Another pair of unstable fixed points, $x_{3,4}^* = \pm \frac{1-a/2}{1-a}$ come into existence for $a > 2$. It is to be noted that as $a \rightarrow 2$ from above, $x_{3,4}^*$ both collide at $x = 0$ causing an interior crisis, which leads to symmetry-breaking of the chaotic attractor.

To observe SR, the value of a was kept close to 2, and then modulated sinusoidally with amplitude δ and frequency ω , i.e.,

$$a_{n+1} = \begin{cases} a_0 + \delta \sin(2\pi\omega n), & \text{if } x \in \text{R} \\ a_0 - \delta \sin(2\pi\omega n), & \text{if } x \in \text{L}. \end{cases} \quad (2)$$

We refer to this henceforth as multiplicative or parametric perturbation, to distinguish it from additive perturbation (discussed later).

The system immediately offers an analogy to the classical bistable well scenario of SR. The sub intervals L and R correspond to the two wells between which the system hops to and fro, aided by the inherent noise (chaos) and the external periodic forcing. In each positive (negative) half-cycle of the periodic signal, a portion of the map defined over R (L) overlaps into the domain of the other portion defined over L (R). This is analogous to the successive raising and lowering of the wells in synchronization with the signal frequency, allowing the system to escape from one well to the other. The resultant intermittent switching of the trajectory between L and R is shown in Fig. 3. If the dynamics of the system due to the internal noise (chaos) has some inherent time-scale (say n_k), as $\frac{1}{\omega} \rightarrow n_k$ the two time-scales may lock onto each other. This resonance should be observable through an increase in the response characteristics of the map.

The response of the system is measured in terms of the normalized distribution of residence times, $N(n)$ [5]. This distribution shows a series of peaks centered at $n_j = (j - \frac{1}{2})n_0$, i.e., odd-integral multiples of

the forcing period, $n_0 = \frac{1}{\omega}$. The strength of the j -th peak

$$P_j = \int_{n_j - \alpha n_0}^{n_j + \alpha n_0} N(n) dn \quad (0 < \alpha < 0.25), \quad (3)$$

is obtained at different values of ω , keeping a_0 fixed for $j=1,2$ and 3. To maximize sensitivity, α was taken to be 0.25. For $a_0 = 2.01$ and $\delta = 0.05$, the response of the system showed a non-monotonic behavior as ω was varied, with P_1 peaking at $\omega_1 \sim 1/400$, a value dependent upon a_0 – a clear signature of SR-type phenomenon. P_2 and P_3 also showed non-monotonic behavior, peaking roughly at odd-integral multiples of ω_1 (Fig. 4(a)).

Similar observations of P_j were done also by varying a_0 keeping ω fixed. Fig. 4(b) shows the results of simulations for $\omega = 1/400$ and $\delta = 0.05$. Here also a non-monotonicity was observed for P_1, P_2 and P_3 . The broadness of the response curve and the magnitude of the peak-strengths are a function of the perturbation magnitude, δ . The variation of P_1 with a_0 for different values of δ were also studied. As δ decreases, the response curve becomes more sharply peaked while the peak-strength decreases.

Note that, the parametric perturbation cannot be done without modulating the noise-intensity. This seems to be the principal difference between this type of ‘chaotic resonance’ and classical SR seems to be. As the local slope of the map, a , is varied periodically, the internal noise, whose intensity is a function of the lyapunov exponent (and hence of a) also varies periodically. In contrast, for classical SR, the wells are raised or lowered periodically without affecting the external noise, which is independent of the geometry of the wells.

Analytical calculations were done to obtain the invariant probability density and the dominant time-scale governing the residence-time distribution. This was done by proper partitioning of the domain of definition of the system and obtaining the eigenvalues of the corresponding transition matrix. From Fig. 2, it is clear that the system spends a longer time in the interval $[-\epsilon/2, \epsilon/2]$, where $\epsilon = a_0 - 2$. So a natural partitioning of the interval $[-1, 1]$ is into the four sub-intervals: $C_1 : [-1, -\epsilon/2]$, $C_2 : [-\epsilon/2, 0]$, $C_3 : [0, \epsilon/2]$ and $C_4 : [\epsilon/2, 1]$. This is an exactly Markov partition at integral values of ϵ , i.e., the partition boundaries, $\{p_i\}$ transform into each other on application of the map dynamics, ($f(p_j) \in \{p_i\}$). It is assumed that for $a_0 \rightarrow 0$ the partitioning approximately retains its Markovian character, so that the process can be mapped onto a Markov process. Close to $\epsilon = 0$, the transition matrix corresponding to the above partitioning is:

$$W = \begin{vmatrix} \frac{1-\epsilon/2-\epsilon^2/4}{1-\epsilon^2/4} & \frac{\epsilon}{4(1-\epsilon^2/4)} & \frac{\epsilon}{4(1-\epsilon^2/4)} & 0 \\ \frac{\epsilon}{2+\epsilon} & \frac{1}{2+\epsilon} & \frac{1}{2+\epsilon} & 0 \\ 0 & \frac{1}{2+\epsilon} & \frac{1}{2+\epsilon} & \frac{\epsilon}{2+\epsilon} \\ 0 & \frac{\epsilon}{4(1-\epsilon^2/4)} & \frac{\epsilon}{4(1-\epsilon^2/4)} & \frac{1-\epsilon/2-\epsilon^2/4}{1-\epsilon^2/4} \end{vmatrix} \quad (4)$$

where, $W_{ij} = P(C_i, C_j)$ is the probability of transition from C_i to C_j . The eigenvalues of the above matrix are $\lambda_1 = 1$, $\lambda_2 = \frac{1-\epsilon/2-\epsilon^2/4}{1-\epsilon^2/4}$, $\lambda_3 = \frac{1-\epsilon}{1-\epsilon^2/4}$ and $\lambda_4 = 0$. The largest eigenvalue, 1, corresponds to the invariant probability density over the four intervals. The next largest eigenvalue dominates any time-dependent phenomena. The relevant time-scale (i.e., the mean residence time) is given by

$$n_k = \frac{-1}{\log(\frac{1-\epsilon/2-\epsilon^2/4}{1-\epsilon^2/4})} \simeq \frac{-1}{\log(1-\epsilon/2)}. \quad (5)$$

So, for $a_0 = 2.01$, $n_k \simeq 200$. This predicts that a peak in the response should be observed at a frequency $\frac{1}{2n_k} \simeq 1/400$, which agrees with the simulation results. For small ϵ , $\lambda_2 \simeq \exp(-\epsilon/2)$. Therefore, as $a_0 \rightarrow 2$ from above, the residence time diverges as

$$n_k \sim (a_0 - a_0^*)^{-1}, \quad a_0^* = 2. \quad (6)$$

The mean time spent by the trajectory in any one of the sub-intervals (L or R) can be calculated exactly for piecewise linear maps [11]. For $\epsilon \neq 0$, the intervals $\beta_1 = (0, \frac{\epsilon}{2(2+\epsilon)})$ and $\beta_2 = [1 - \frac{\epsilon}{2(2+\epsilon)}, 1]$ of R maps to L, so that the trajectory escapes from one sub-interval to the other. Note the symmetrical placement of the two R \rightarrow L ‘escape regions’ about $x = 0.5$, because of the symmetry $F(1/2 - x) = F(1/2 + x)$ of the DAT map. So the total fraction of R escaping to L after one iteration is $l_1 = \frac{2\epsilon}{2(2+\epsilon)}$. Let us now consider the first pre-image of β_1 and β_2 , which escapes from R to L after two iterations. The total fraction of R belonging to this set is $l_2 = \frac{4\epsilon}{2(2+\epsilon)^2}$. Proceeding in this manner, we find from the geometry of the map that the total fraction of R which maps to L after n iterations is

$$l_n = \frac{2^n \epsilon}{2(2+\epsilon)^n}. \quad (7)$$

These are just the probabilities that the trajectory spends a period of n iterations in R before escaping to L ($\sum_{j=1}^{\infty} l_j = 1$). So the average lifetime of a trajectory in R is

$$\langle n \rangle = \sum_{j=1}^{\infty} (j-1) l_j = \frac{2}{\epsilon}. \quad (8)$$

For $a_0 = 2.01$, $\langle n \rangle = 200$, in good agreement with the result obtained using the approximate Markov partitioning. The above equation also establishes exactly the linear scaling relation of the mean lifetime about $\epsilon = 0$, with $\langle n \rangle$ diverging at $a_0 = 2$. By symmetry of the map, identical results will be obtained if we consider the trajectory switching from L to R.

Another interesting quantity which also shows a scaling behavior around $\epsilon = 0$, is the drift rate, v , from one sub-interval to the other [12]. This measures the rate at which the chaotic trajectory switches between L and R. Owing to the symmetry $F(-x) = -F(x)$ of the DAT map, the net drift rate is zero, i.e., switching to either sub-interval occurs equally often. Let us consider switching from R to L (identical results will hold for switching in the opposite direction due to symmetry). The drift rate is measured by the fraction of R mapping to L per iteration. Hence,

$$v = \frac{\epsilon}{2+\epsilon}. \quad (9)$$

It is again a linear scaling relation as $a_0 \rightarrow 2$ from above. Note that, $a_0 < 2$, $v = 0$ as the two sub-intervals are isolated from each other. Thus v is analogous to an ‘order parameter’, having a finite (positive) value above $a_0 = 2$ and zero below it. This suggests that the merging of the chaotic attractors at $a_0 = 2$ is akin to a critical phenomena, with the local slope a_0 as the tuning parameter.

Similar study was also conducted with additive perturbation for the above map. In this case the dynamical system is defined as follows:

$$x_{n+1} = F(x_n) + \delta \sin(2\pi\omega n). \quad (10)$$

For $a = 1.9$ (say), the map has two disconnected sub-intervals, L:[-1,0) and R:(0,1]. However, an additive perturbation of magnitude $\delta > 0.1$ causes a portion of L to diffuse into R in the positive half-cycle of the sinusoidal signal (of frequency ω). Similarly, in the negative half-cycle, a portion of the R interval diffuses into L. The long-term behavior of the map is described by a “smeared-out” DAT map with a width δ rather than the “crisp” piecewise linear DAT map with $a_0 = 1.9$. This happens as the map performs a periodic vertical motion, causing a smearing-out over time. The simulation results showed non-monotonic behavior for the response as either ω or a_0 was varied, keeping the other constant, but this was less marked than in the case of multiplicative perturbation. This work can be seen in context with studies conducted on the dynamics of the logistic map under parametric perturbation [13].

Low-dimensional discrete-time dynamical systems are amenable to several analytical techniques and hence can be well-understood compared to other systems. The examination of resonance phenomena in this scenario was for ease of numerical and theoretical analysis. However, it is reasonable to assume that

similar behavior occurs in higher-dimensional chaotic system, described by both maps and differential equations.

The close resemblance of the merging of attractors with critical phenomena has possible relevance to SR in Ising systems. Although numerical studies have reported SR in kinetic Ising system, it seems to be inconclusive as the primary peak strength of the normalized residence-time distribution shows only a monotonic behavior [14]. This response profile is identical to that observed in DAT Map for $a_0 < 2$. A study of kinetic aspects like hysteresis is planned to be undertaken, which should give information concerning the phase-dependence of the resonance behavior.

The observation of ‘SR’ in chaotic systems also has implications for the area of noisy information processing. It has been proposed that the sensory apparatus of several creatures use SR to enhance their sensitivity to weak external stimulus, e.g., the approach of a predator. Some experimental work on crayfish have provided supporting evidence to this assertion [15]. The above study indicates that external noise is not necessary for such amplification as chaos in neural networks can enhance weak signals. As chaotic behavior is extremely common in a recurrent network of excitatory and inhibitory neurons, such a scenario is not entirely unlikely to have occurred in the biological world. This can however be confirmed only by further biological studies and detailed modeling of the phenomena.

Several interesting comments on the work were made by Prashant M. Gade (JNCASR, Bangalore). Jayanta K. Bhattacharjee (IACS, Calcutta) made some useful suggestions.

Figure Captions

Fig. 1 The DAT map for $a_0 = 2.01$. Inset: a magnified view of the map in the interval $[-0.005, 0.005] \times [-0.005, 0.005]$.

Fig. 2 Attractor of the DAT map versus a_0 . The figure was obtained for $x_0 \in R$. For $x_0 \in L$ the corresponding image is obtained by reflecting about x -axis.

Fig. 3 The time-evolution of the sinusoidally perturbed DAT map for $a_0 = 2.01$, $\omega = 1/400$ and $\delta = 0.05$. The broken line is the boundary between L and R.

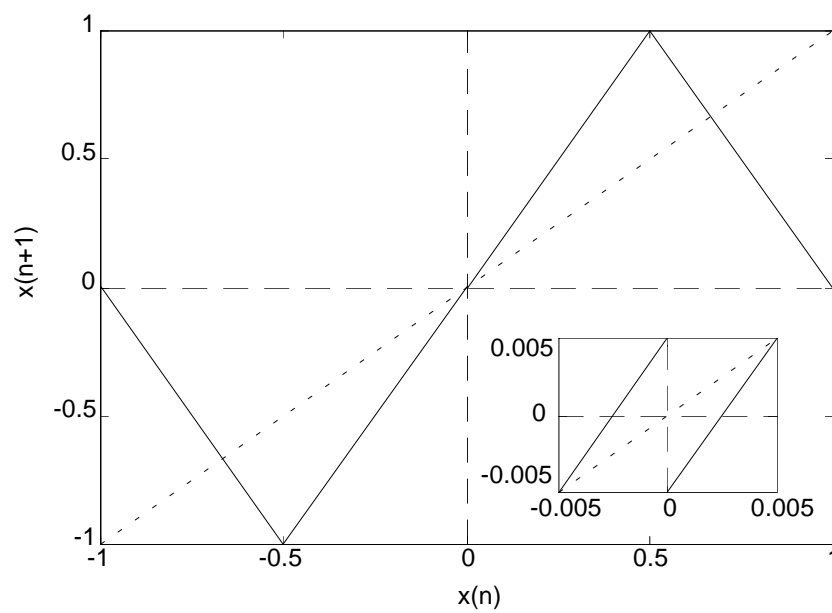
Fig. 4 (a) P_n ($n = 1, 2, 3$) versus ω for $a_0 = 2.01$ and $\delta = 0.05$, (b) P_n ($n = 1, 2, 3$) versus a_0 for $\omega = 1/400$ and $\delta = 0.05$. The circles represent the average value of P_n for 18 different initial values of x , the bars representing the standard deviation. The data points are joined by solid lines for the reader’s convenience.

References

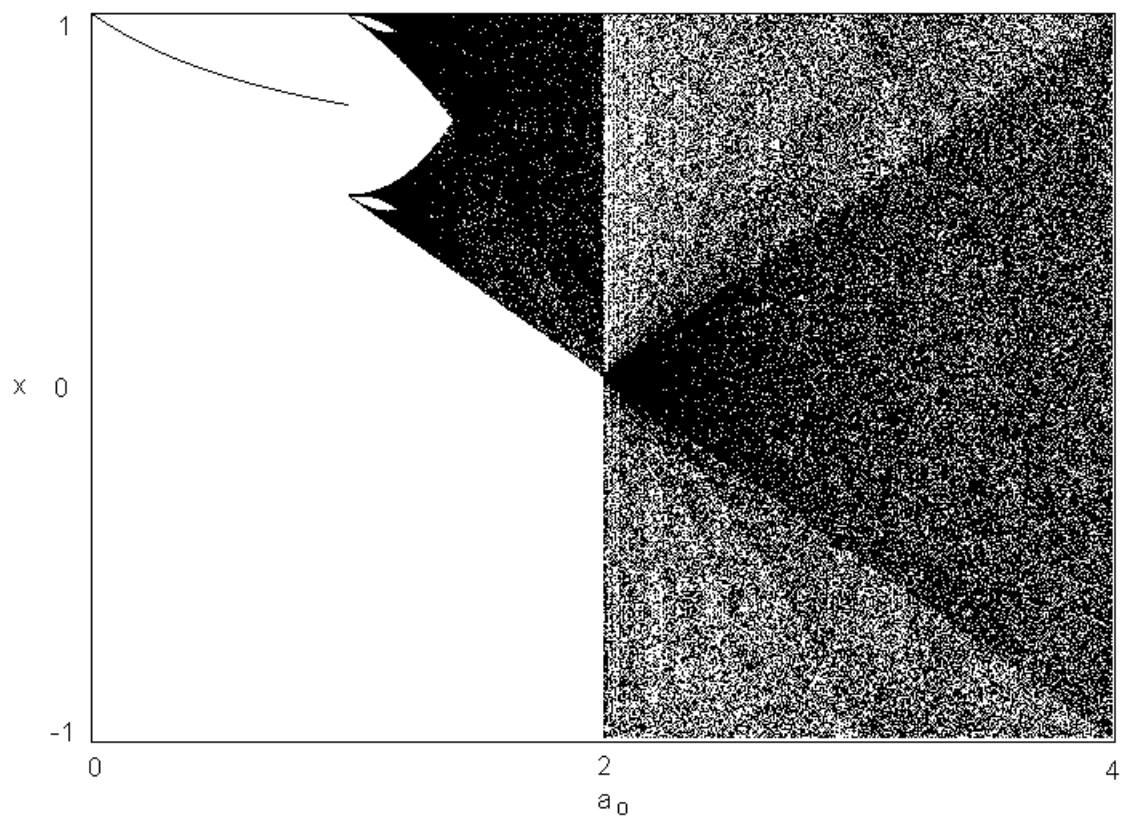
- [1] R. Benzi, A. Sutera and A. Vulpiani, *J. Phys. A* **14**, L453 (1981).
- [2] B. McNamara and K. Wiesenfeld, *Phys. Rev. A* **39**, 4854 (1989).
- [3] G. Nicolis, C. Nicolis and D. McKernan, *J. Stat. Phys.* **70**, 125 (1993).
- [4] V. S. Anishchenko, A. B. Neiman and M. A. Safanova, *J. Stat. Phys.* **70**, 183 (1993).
- [5] L. Gammaitoni, F. Marchesoni and S. Santucci, *Phys. Rev. Lett.* **74**, 1052 (1995).

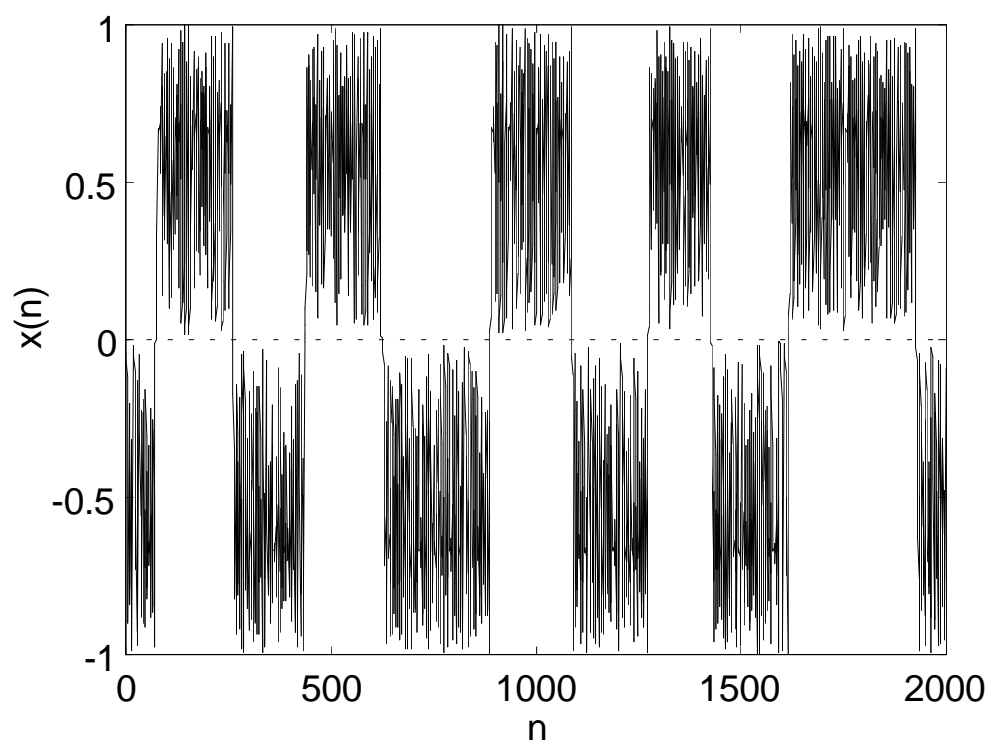
- [6] E. Ippen, J. Lindner and W. L. Ditto, *J. Stat. Phys.* **70**, 437 (1993).
- [7] T. L. Carroll and L. M. Pecora, *Phys. Rev. Lett.* **70**, 576 (1993).
- [8] R. M. May, *Ann. N. Y. Acad. Sci.* **316**, 517 (1979); J. Testa and G. Held, *Phys. Rev A* **28**, 3085 (1983).
- [9] P. M. Gade, R. Rai and H. Singh, *preprint* ([http:// xxx.lanl.gov/abs/chao-dyn/9704010](http://xxx.lanl.gov/abs/chao-dyn/9704010)) (1997).
- [10] C. Seko and K. Takatsuka, *Phys. Rev. E* **54**, 956 (1996).
- [11] R. M. Everson, *Phys. Lett. A* **122**, 471 (1987).
- [12] S. Grossman and H. Fujisaka, *Phys. Rev. A* **26**, 1779 (1982).
- [13] P. P. Saratchandran, V. M. Nandakumaran and G. Ambika, *Pramana - J. Phys.* **47**, 339 (1996).
- [14] S. W. Sides, R. A. Ramos, P. A. Rikvold and M. A. Novotny, *preprint* ([http:// www.aps.org/BAPSMAR96/abs/S3090009.html](http://www.aps.org/BAPSMAR96/abs/S3090009.html)) (1996); *J. Appl. Phys.* **81**, 5597 (1997).
- [15] J. K. Douglass, L. Wilkens, E. Pantazelou and F. Moss, *Nature* **365**, 337 (1993).

Sinha et al
Figure 1



Sinha et al
Figure 2





Sinha et al
Figure 4

